EVALUATING COPPER ISOTOPE FRACTIONATION IN THE METALLURGICAL OPERATIONAL CHAIN: AN EXPERIMENTAL APPROACH*

S. KLEIN†

Forschungsbereich Archäometallurgie, Deutsches Bergbau-Museum Bochum (DBM), Am Bergbaumuseum 31 D-44791 Bochum, Germany and FIERCE, Frankfurt Isotope & Element Research Center, Goethe Universität, Altenhöferallee 1 D-60438 Frankfurt am Main, Germany

T. ROSE

Department of Bible, Archaeology and Ancient Near East, Ben-Gurion University of the Negev, Be'er Sheva, Israel and Department of Antiquity, Sapienza University of Rome, Rome, Italy

Until today, raw material information of copper (Cu) objects is mostly gained from impurities and trace elements and not from the Cu itself. This might be obtained using its stable isotopes. However, isotopic fingerprinting requires the absence of fractionation during the smelting process. The Cu isotope evolution during outdoor smelting experiments with Cu sulphide ore was investigated. It is shown that external materials, in particular furnace lining, clay, manure and sand, alter the isotopic composition of the smelting products. Cu isotopes are fractionated within low viscosity slag derived from matte smelting. The produced metallic Cu has a Cu isotope signature close to the ore.

KEYWORDS: COPPER ISOTOPES, FRACTIONATION, CHAÎNE OPÉRATOIRE, ORE, SLAG, MATTE, MASS SPECTROMETRY

INTRODUCTION

The first analytical approaches to measuring the natural Cu isotope abundances appear far before the development of modern mass spectrometers (Ewald 1944; Brown and Inghram 1947). Measurement of Cu isotopes was established by Walker *et al*. (1958) and immediately applied to understand the variations in (Cu) minerals and possible natural fractionation effects (White *et al*. 1962; Shields *et al*. 1965). This became more common with the introduction of multi-collector inductively coupled plasma-mass spectrometry (MC-ICP-MS) in Cu isotope analysis by Maréchal *et al*. (1999). Research is still dominated by the study of natural variation of Cu isotopes in geological material (Zhu *et al*. 2000; Albarède 2004; Albarède and Beard 2004; Asael 2010; Mathur and Wang 2019), but also includes other materials such as extra-terrestrial materials (Moynier *et al*. 2006, 2007; Herzog *et al*. 2009), native Cu (Dekov *et al*. 2013), pollution and contamination (Albarède and Beard 2004; Borrok *et al*. 2008), rivers and oceans (Vance *et al*. 2008), oxidative weathering (Fernandez and Borrok 2009; Mathur and Fantle 2015), or soils and interaction with micro-organisms (Mathur *et al*. 2005; Pokrovsky *et al*. 2008; Bigalke *et al*. 2010), next to others (cf. Moynier *et al*. 2017).

*Received 10 October 2019; accepted 24 March 2020
†Corresponding author: email sabine.klein@bergbaumuseum.de
The peer review history for this article is available at https://publons.com/publon/10.1111/arcm.12564
[Correction added on 18 May 2020, after first online publication: Peer review history statement has been added.]

Cu isotopes were initially suggested as a possible tool in metal provenance studies by Gale and Stos-Gale (1982) and explored first by Gale *et al*. (1999) and Woodhead *et al*. (1999) to link objects to raw metal sources (Artioli *et al*. 2008). Since then, Cu isotopes were used several times to trace the ore provenance (e.g., Mathur *et al*. 2009a, b, c; Desaulty *et al*. 2011; Bower *et al*. 2013; Bugaj *et al*. 2019; Reguera-Galan *et al*. 2019). However, it has been observed that Cu isotopes indicate rather the ore type within a deposit than the location of the ore deposit, and thus are complementary to Pb isotopes (Klein *et al*. 2010; Mathur and Fantle 2015; Powell *et al*. 2017; Jansen *et al*. 2018). Cu isotopes were also applied to the provenance of turquoise (Hull *et al*. 2014) and glass (Lobo *et al*. 2014).

For metal provenance studies, a direct link between the metal and the ore as a representative of the geological setting and the ore formation process is fundamental (e.g., Klein *et al*. 2010; Jansen 2011). To establish this link, the fractionation of Cu isotopes during all steps of the metallurgical process from ore to withdrawn metal must be considered. Gale *et al*. (1999) were the first to analyse products of smelting and re-firing experiments for Cu isotope analysis. They concluded that no fractionation occurs during these processes, but emphasized the need for further study. Bower *et al*. (2013) confirmed the hypothesis of Gale *et al*. (1999) that no Cu isotope fractionation occurred during the smelting processes. All other Cu isotope studies concerning archaeometallurgical materials referred to Gale *et al*. as the evidence for a direct link between ore and metal (e.g., Klein *et al*. 2004; Klein *et al*. 2010; Desaulty *et al*. 2011).

This is remarkable as Gale *et al*. (1999) have not provided comprehensive closure. Their study was rather meant to fuel future studies. They were well aware that their approach had limitations because only oxide ores were analysed. Oxide ores do not reflect the prehistoric procedures and smelting processes in their entirety, because sulphide ores were already exploited for Cu smelting in the Early Bronze Age (Hauptmann *et al*. 1985; Hauptmann 1989). Because of the sensitivity of Cu isotopes to reductive and oxidative reactions, in particular the partial oxidation during roasting of naturally more common sulphide Cu ore may cause significant fractionation. This has already been confirmed for low-temperature alteration of primary Cu sulphides (Asael *et al*. 2007; Asael 2010; Mathur and Fantle 2015). The different behaviour of the reduced and oxidized phases during smelting may further shift the isotopic signature, which has been already altered through the roasting of the original ore. Additionally, Bower *et al*. (2013) used reagent-grade $CuCO_3$ only, instead of natural ore, which is not reflecting the situation in prehistoric times. The contribution of the different influences during the smelting process on stable isotope fractionation was assessed with laboratory experiments using small amounts of pure malachite (Rose *et al*. 2017). Owing to impurities in natural ores, a certain amount of slag is always present within the smelting products. Only rarely was Cu completely removed from the silicates (ore and slag); hence, isotope fractionation could occur due to the different binding environments in slag, matte and metal. Another limitation of Gale *et al*. (1999) is the early stage of the analytical methods available. They report analytical errors of up to 0.48‰, which is more than double the typical analytical errors in Cu isotope analysis today (< 0.14‰ 2σ). Therefore, the elder method made it almost impossible to detect fractionation. Last but not least, the authors had not provided the reader with detailed descriptions of the experiments, so that their experiments were not replicable. Consequently, a systematic approach is still missing in this important field after 20 years of research.

To implement such a systematic approach, various factors have to be considered. It is known that Cu isotope fractionation is strongly influenced by redox processes, that is, reactions which change the oxidation state of Cu (Moynier *et al*. 2017). The behaviour of Cu isotopes can be roughly predicted by the principles of stable isotope fractionation theory (Schauble 2004).

According to it, fractionation during redox reactions results in an enrichment of the heavier isotope ^{65}Cu in the oxidized Cu phases, for example, in the slag. This is confirmed by several studies that investigated the fractionation between sulphide and silicate melts in the mantle (Savage *et al*. 2015; Huang *et al*. 2017; Zhao *et al*. 2017). Cu isotopes of mantle magma sulphides may be contaminated with crustal (siliceous) rocks (Zhu *et al*. 2000). Although the geological settings differ, all showed that ^{65}Cu is enriched in the silicate phases during melting of sulphides.

Accordingly, smelting of Cu sulphides with its several cycles of partial oxidation of Cu during roasting followed by the separation of reduced and oxidized Cu phases during smelting should provide ideal conditions for pronounced Cu isotope fractionation. Density segregation and differences in the binding environment and the surface tension of metal, matte and slag could amplify this fractionation because they might prevent the exchange between the different Cu phases. The high temperature necessary for smelting may dampen this effect, because rising temperatures decrease isotope fractionation (Schauble 2004), but its extent is unknown.

AIMS

This study aims to establish the first systematic approach to Cu isotope fractionation during the smelting process. Based on Cu oxide and sulphide smelting experiments in shaft furnaces, pit furnaces and crucibles, designed according to the reconstructed prehistoric Cu smelting process, the potential of Cu isotopes as a tool in archaeometallurgical research was systematically evaluated.

To reach this goal, the project design consists of three parts. First, smelting experiments at the Laboratory for Experimental Archaeology (LEA) in Mayen, Römisch-Germanisches Zentralmuseum (RGZM Mainz), were carried out. Second, the material withdrawn during the experiments was analysed by inductively coupled plasma-mass spectrometry (ICP-MS), MC-ICP-MS, electron probe microanalysis (EPMA) and X-ray diffraction (XRD) for their elemental composition, Cu isotope composition, and mineralogical phases in order to quantify the partitioning of Cu and possible changes in Cu isotope composition. In a final step, which is not the subject of this paper, the analyses will be combined in a mass-balance model. This will allow the identification of fractionation factors for Cu isotopes throughout the operational chain and the establishment of fractionation factors between silicates (slag), Cu metal, roasted and unroasted Cu ore.

SMELTING EXPERIMENTS

The smelting experiments were set up according to the reconstruction of prehistoric smelting processes in crucibles (e.g., between the fifth and fourth millennia BCE of the Near East—Hauptmann 2007; and in the Mitterberg region during the second half of the second millennium BCE —Hanning and Pils 2011) with pure malachite and chalcopyrite ore, respectively. The shaft furnace and roasting hearths were built according to the excavated remains. Malachite ore was smelted directly in pit furnaces and crucibles; the chalcopyrite ore was smelted in a shaft furnace. All experiments were conducted with the closest proximity to the archaeological reconstructions possible. All process parameters were documented *in situ*. Temperature was monitored continuously with thermocouples. All materials used in and produced by the experiments were sampled and analysed. Small-scale variations ($> 1‰$ in a few millimetres) are well known in Cu ores (e.g., Markl *et al*. 2006; Mathur et al. 2009a, b), but homogenization of the used ore was achieved before smelting by crushing and grinding the solid material in a larger amount. Heterogeneity may occur in the smelting products due to the heterogeneous conditions within the furnace (temperature, atmosphere) or the assimilation of external material such as the furnace lining.

Therefore, several samples were taken from the smelting products (slag, matte). In order to minimize random effects, four shaft furnace experiment series (labelled S1–S4) were carried out with roasted and homogenized chalcopyrite ore. In the shaft furnace, sulphide-rich matte was the main smelting product carrying Cu, which after withdrawing it from the furnace was crushed, ground and kneaded with manure to form pellets. These pellets were then roasted and smelted a second time in either a pit furnace or a graphite crucible with a lid in a hearth. Sometimes it needed even more than one sequence until pure Cu metal was extractable as a regulus. For a detailed description of the experiment series, installations, chemicals used, parameters, etc., see Rose *et al*. 2019, 2020.

In the following, the two most successful ones of the four shaft furnace experiment series (S2 and S4) are presented, thus allowing the most detailed interpretation of their Cu isotope behaviour along the operational chain ('chaîne opératoire'). Shaft experiment series S2 and S4 started with the smelting of sulphide ore in the self-constructed shaft furnace. The sulphide ore was roasted before the charging. The (semi-)products from the furnace smelting (slag and matte) were then separated, crushed, roasted, processed and re-smelted in pit furnaces (p) or crucibles (c) in order to increase stepwise the gain of the Cu metal.

METHODS

Polished sections of the ores, roasted ores, matte and slag were produced for optical microscopy and EPMA. Powdered material of ore, matte and slag samples were crushed, ground and parted for complete homogenization of the solid material (Ney 1986). Wet chemistry procedures were carried out in the clean laboratories of the Deutsches Bergbau-Museum Bochum (DBM) (elemental analysis preparation) and FIERCE (column separation for isotope analysis). Millipore® water, quartz-distilled and double-distilled acids, and bleached polytetrafluoroethylene (PTFE) beakers were used throughout the analytical processes. For more detailed information, see Rose *et al*. (2020).

Cu ion-exchange chromatography was applied to separate Cu from Fe and other elements based on the protocol of Maréchal *et al*. (1999). Unwanted isotope fractionation may occur from the procedure because of the incomplete recovery of Cu (Maréchal and Albarède 2002; Mason *et al*. 2004; Fujii *et al*. 2013). Further suggestions for improvements were proposed by Albarède *et al*. (2015). Calibration of the columns is a crucial requirement (Maréchal *et al*. 1999; Petit *et al*. 2008), even more because of the specific chemistry of the ore and smelting products. The separated Cu solution was then evaporated and diluted in 1 ml 2% HNO_3 with 250 ppb Ni (NIST SRM-986; Ehrlich *et al*. 2004). Cu isotope analysis was performed with a ThermoScientific NeptunePlus MC-ICP-MS at FIERCE. Chemical blanks were measured at the beginning of each sequence to monitor the pureness of the acids. For mass bias correction, the sample-standard bracketing method (Zhu *et al*. 2000; Larson *et al*. 2003; Peel *et al*. 2008) was used. Three samples each were bracketed in the Cu standard NIST SRM-976. The internal background was corrected with blank measurements. NIST SRM-976 was monitored as an unknown sample for quality proof. The Cu isotope results are presented as δ^{65}Cu values. The elemental composition of all materials was measured quantitatively with the ICP-MS at the DBM. For a full description of the applied analytical methods, see Rose *et al*. (2020).

Smelting materials

The chalcopyrite ore used for the experiments was collected from the Mitterberg mining district (St. Johann im Pongau, Austria) by E. Hanning as part of her doctorate work, and made available

for the experiments. The ore is of hydrothermal genesis (Bernhard 1965). The pieces were sampled directly from the centre of the primary ore body.

Sulphide ore and roasted ore Hydrothermal chalcopyrite-rich ore is by nature a paragenesis of Cu and Fe sulphide phases, and is usually associated with silicate-rich gangue material. The chalcopyrite ore used in the experiments was identified by XRD as an intergrowth of chalcopyrite ($CuFeS_2$) together with pyrite (FeS_2), quartz (SiO_2), diopside ($CaMgSi_2O_6$) and phlogopite ($K_2(Mg,Fe)_2(OH)_2(AlSi_3O_{10})$). Crushing of the ore was carried out in the smelting site with a hammer and stone anvil, guaranteeing complete homogenization. The crushed ore was roasted in an open fire bed (Rose *et al*. 2019) under oxidizing conditions to convert the sulphide minerals into a mixture of Cu oxides, Fe oxides and sulphide phases. The roasted ore had a porous structure.

Identified with XRD were chalcopyrite ($CuFeS_2$), bornite (Cu_5FeS_4), cubanite ($CuFe_2S_3$), chalcocite (Cu_2S), pyrite (FeS_2), magnetite (Fe_3O_4), hematite (Fe_2O_3) and quartz. Additional, secondary phases such as kieserite ($MgSO_4{\cdot}H_2O$) occurred, which presumably formed either during rapid water cooling as applied in the roasting procedure or later because of a reaction with air moisture.

Sulphide-rich matte Solidified Cu matte (German: *Kupferstein*) is the major semi-product that collects the Cu in a first stage, needing further smelting in order to yield Cu metal. It consists of chalcocite (Cu_2S) with a variable contribution of FeS within the ternary system of Cu-Fe-S (for the great variety of Cu-Fe sulphide phases, which can form in Cu mattes, see Lechtman and Klein 1999). It contains roughly 70% Cu. The matte typically has a de-mixed structure and either crystallizes in a blocky structure with brownish to greyish stains and internal de-mixed components or as microstructural lamellae. In pores and cracks, pure Cu filaments (whisker Cu) had formed. In intergranular regions, feathery structures occurred, as described by Lechtman and Klein (1999). According to XRD analysis, inclusions were of a variety of phase compositions. Dendritic magnetite (Fe_3O_4), Fe and Cu occurred as reduced phases, and sulphide remains were identified as chalcocite, covellite (CuS), valleriite ($2((Fe,Cu)S){\cdot}1.53(Mg,Al)(OH)_2$), troilite (FeS) and millerite (NiS). Silicate components including slag remains were comprised of fayalite, forsterite (Mg_2SiO_4), ferrosilite ($(Fe,Mg)_2Si_2O_6$), hedenbergite ($CaFeSi_2O_6$), quartz and its high-temperature modification cristobalite.

Slag Slag is partly glassy or shows an elongated crystal structure. The microstructures reflect homogenization of the smelting components. Pyroxenes and fayalite were the major slag phases in experiments S2 and S4, and if fayalite has crystallized, it occurred as skeletal laths and polyhedral hopper olivines (Erdmann *et al*. 2014), indicating initial cooling rates between 15 and 40° C/h (Arndt and Fowler 2004). With XRD analysis, diopside ($CaMgSi_2O_6$), hedenbergite ($CaFeSi_2O_6$), quartz and cristobalite, magnetite as inclusions, and ferrosilite ($(Fe,Mg)_2Si_2O_6$) were also identified. Metallic Cu prills and globular matte inclusions with typical de-mixing lamellae were distributed throughout the slag.

The main chemical composition of all materials used and produced in the experiments is presented in Table 1. For more detailed information, see Rose *et al*. (2020).

Table 1 *Main elemental composition of the materials and smelting products measured by inductively coupled plasma-mass spectrometry (ICP-MS) (DBM). Values are in weight percentage (wt%); for copper, the complete concentration range is given; for all other element values > 2 wt% are listed. For complete minor and trace element composition, see Rose et al. (2020).*

Sample ID	*Material*	*Cu*	*Fe*	*S*	*SiO_2*	*TiO_2*	*Al_2O_3*	*CaO*	*MgO*	*K_2O*
Raw material										
Cpy6	Chalkopyrite ore, Arthurstollen, St. Johann im Pongau (Austria)	21.0	22.7	24.3	29.2					
Wood	Soft wood	< 0.005								
Clay	Clay	0.31			63.6		12.7	3.9		
Dung	Manure	< 0.005								
Charcoal dust	Charcoal	0.34	10.2		12.9		4.0	6.3		2.6
Sand	Sand	0.08			93.8					
Roasted ore										
R11f	Small grains of leached roasted ore	13.8	35.6	6.3	32.3		4.2	2.3		
R11l	Liquid with which R11f reacted for several months	11.7		8.5					2.2	
R21f	Small grains of leached roasted ore	25.9	35.1	20.3	16.0			2.8		
R21l	Liquid with which R21f reacted for several months	0.80		4.7					5.5	
R28	Bulk sample of the quench liquid	12.8	4.8	18.0				4.8	3.6	6.0
R-bulk	Bulk sample	20.5	35.5	16.2	24.9			2.8		
R-bulk-ox	Bulk sample enriched in oxidized material	12.1	38.2	7.8	31.4			6.4	3.8	
R-bulk-red	Bulk sample enriched in reduced/unroasted material	28.3	31.6	21.0	21.1					
Experiment series S2										
S2f1-m	Matte, bulk sample	28.3	30.0	18.3	15.8			2.2		
S2f1-s	Slag, bulk sample	10.0	19.3	6.5	49.5		3.6	4.2		
S2r1-rm	Roasted matte	54.6	25.8	21.3	2.6					
S2p1a-cp	Copper prills	67.2	13.2	11.6						
S2p1a-m	Matte	54.3	17.9	19.0	7.7					
S2p1a-s-1	Platy slag (melt quenched with water and extracted)	2.6	22.1		57.8		4.2	5.0	2.0	2.2
S2p1a-s-2	Massive slag (melt cooled down in pit furnace)	4.2	37.6		39.0		3.4	5.3	2.1	
S2p1a-sm	Mixture of slag and matte	22.6	30.6	7.5	28.4		2.3	3.4		
S2p1b-sc-4	Copper prill, extracted from slag cake	92.5	3.2							

(*Continues*)

Table 1 *(Continued)*

Sample ID	*Material*	*Cu*	*Fe*	*S*	*SiO_2*	*TiO_2*	*Al_2O_3*	*CaO*	*MgO*	*K_2O*
S2p2-sm-m	Matte close to slag, crushed from same piece as S2p2-sm-s	51.8	17.7	19.1	9.2					
S2p2-sm-s	Slag close to matte, crushed from same piece as S2p2-sm-m	2.3	31.9		44.8		4.1	6.3	2.6	2.4
S2p2-sm-um	Unreacted matte	21.7	25.7	7.3	26.6		2.4	3.4		
S2p3-cp	Copper prill	94.9	4.1							
S2p3-m	Matte	59.0	16.0	21.8						
S2p3-s	Slag	19.8	25.0	6.9	34.0		4.3	5.0		2.1
S2p3-fm	Mixed material, too small to separate	27.8	29.8	9.3	26.0		2.8	4.2		
S2p3-cc	Unburnt charcoal after experiment	2.6								
S2p3c1-m	Matte	56.1	18.1	20.0	2.8					
S2p3c1-s	Slag	3.0	27.7		48.0		4.3	6.7	2.3	2.6
S2p3c2-m	Matte	55.4	19.0	22.4						
S2p3c2-s	Slag	26.3	39.1	3.4	31.9					
S2p3c3-m	Matte	58.2	16.3	21.9	2.0					
S2p3c3-s	Slag	3.2	32.4		42.8		3.6	8.5	2.6	2.9
S2p3c4-cu	Copper regulus	98.7								
S2p3c4-m	Matte	73.9		18.0	2.0					
S2p3r1-rm	Roasted matte	52.4	23.8	16.9	8.2					
S2p3c4-s-1	Slag	7.4	39.7		43.4			3.3		
S2p3c4-s-2	Copper prills in slag sample S2p3c4-s-1	12.3	7.0	3.6	3.2		2.5	7.0		2.2
Experiment series S4										
S4f1-cc	Charcoal leftover in furnace	0.033								
S4f1-cp	Copper prills	7.4	59.9							
S4f1-m	Matte, bulk sample	22.8	27.0	16.0	22.0			2.5		
S4f1-m2-1	Matte	40.1	31.2	23.7						
S4f1-m2-2	Copper hair grown on sample S4f1-m2-1	90.6								
S4f1-m4	Matte	37.7	32.2	22.5						
S4f1-s	Slag	3.3	12.0		71.5			3.7		
S4f1-sm	Mixture of slag and matte	11.6	20.6	6.8	48.1		2.4	4.7	2.2	
S4f1-fm	Mixed material, too small to separate	15.4	29.1	11.5	34.0		6.4	2.4		
S4f1-uo	Unreacted ore	16.4	29.5	13.6	32.2			6.4	3.3	
S4f1-fl1-1	Furnace lining	0.33	3.3		68.5		18.4	3.1		2.2
S4f1-fl1-2	Furnace lining	0.27	3.1		77.6	2,1	9.7	2.4		
S4f1-fl2-1	Furnace lining	36.6	43.6	22.7	2.3					
S4f1-fl2-2	Furnace lining	0.10	3.1		66.9	2,3	20.5	3.0		
S4r1-rm	Roasted matte	23.1	33.0	11.3	25.7			2.8		
S4p1-cp	Copper prills	82.2	5.2	2.0						
S4p1-m-1	Matte	57.5	14.1	22.1						

(*Continues*)

Table 1 *(Continued)*

Sample ID	*Material*	*Cu*	*Fe*	*S*	*SiO_2*	*TiO_2*	*Al_2O_3*	*CaO*	*MgO*	*K_2O*
S4p1-m-2	Copper sponge	83.8	14.5							
S4p1-m-4	Copper prill	28.4	60.2	2.6						
S4p1-fm	Mixed material, too small to separate	30.2	23.5	9.4	20.2		2.2	3.3		
S4p1-cc	Unburnt charcoal after experiment	0.009								
S4p1-s2	Platy slag (melt quenched with water and extracted)	0.95	28.8		47.2		4.4	10.1	3.0	3.3
S4p1-s4	Platy slag (melt quenched with water and extracted)	15.8	25.4	4.4	49.6			2.2		
S4p1-sm-1	Slag in direct contact with matte (quenched)	5.1	31.1		42.1		3.8	9.2	2.7	3.2
S4p1-sm-2	Mixture of slag and matte from the same piece such as S4p1-sm-1	0.80	31.4		43.8		3.9	9.1	2.8	3.3
S4p2-m	Matte	49.0	22.8	15.5	4.4					
S4p2-s	Slag	11.2	26.5	4.2	36.5		4.0	8.3	2.5	2.4
S4p2-fm	Mixed material, too small to separate	31.1	19.6	9.9	22.9			3.0		
S4p2c1-cu	Copper regulus	79.5	13.7							
S4p2c1-m	Matte	56.2	15.1	20.7	6.6					
S4p2c1-s	Slag	19.9	25.4	3.6	35.8		2.5	4.9		
S4p2r1-rm	Roasted matte	56.7	24.0	22.2						
S4p2c2-s	Slag	3.7	45.0		44.9			2.2		
S4p2c2-sm	Matte close to slag	63.0	12.9	19.9						
S4p2c3-cu-1	Copper prill	98.5								
S4p2c3-cu-2	Copper regulus	98.1								
S4p2c3-sm	Matte close to slag	65.7	3.1	18.1						
S4p2c3-s	Slag	10.2	54.0		25.7			2.9		

RESULTS OF CU ISOTOPE MEASUREMENTS

The presented experiments concentrate on the two chalcopyrite experiment runs S2 and S4 in the shaft furnace, followed by pit furnace or crucible smelting. Sample numbering was designed as follows: S = sulphide ore, f = furnace, p = pit and c = crucible. The starting materials and smelting products were considered for Cu isotope analysis: furnace lining (fl), charcoal (cc), wood, manure, natural (cpy) and roasted ore, matte (m), roasted matte (rm), slag (s), and produced Cu metal as larger piece (cu) or prills (cp). The Cu isotope results are listed in Table 2. Wherever no fractionation effect occurred, all materials within a single experiment had δ^{65}Cu signatures very close to each other. In the following detailed description, the focus will lie on such samples, which do not follow this rule.

Table 2 *δ^{65}Cu-values for all materials and experiments measured by MC-ICP-MS (FIERCE Laboratory, Frankfurt). Analytical precision (2σ) for all samples is 0.16‰.*

Sample ID	*Material*	*δ^{65}Cu*
Raw material		
Cpy6	Chalkopyrite ore, Arthurstollen, St. Johann im Pongau (Austria)	0.46
Wood	Soft wood	0.49
Clay	Clay	−1.40
Dung	Manure	0.02
Charcoal dust	Charcoal	0.60
Sand	Sand	7.25
Roasted ore		
R11f	Small grains of leached roasted ore	−0.26
R11l	Liquid with which R11f reacted for several months	1.86
R21f	Small grains of leached roasted ore	−0.03
R21l	Liquid with which R21f reacted for several months	1.40
R28	Bulk sample of the quench liquid	0.92
R-bulk	Bulk sample	0.18
R-bulk-ox	Bulk sample enriched in oxidized material	0.41
R-bulk-red	Bulk sample enriched in reduced/unroasted material	0.38
Experiment series S2		
S2f1-m	Matte, bulk sample	0.44
S2f1-s	Slag, bulk sample	0.23
S2f1-sc-1	Matte, drilled from furnace conglomerate	0.13
S2f1-sc-2	Matte, drilled from furnace conglomerate	−0.04
S2f1-sc-3	Matte, drilled from furnace conglomerate	0.11
S2f1-sc-4	Matte, drilled from furnace conglomerate	0.16
S2f1-sc-5	Matte, drilled from furnace conglomerate	0.22
S2f1-sc-6	Slag, drilled from furnace conglomerate	−0.23
S2f1-sc-7	Slag, drilled from furnace conglomerate	0.23
S2f1-sc-8	Slag, drilled from furnace conglomerate	−0.13
S2f1-sc-9	Slag, drilled from furnace conglomerate	−0.28
S2r1-rm	Roasted matte	−0.01
S2p1a-cp	Copper prills	0.64
S2p1a-m	Matte	0.19
S2p1a-s-1	Platy slag (melt quenched with water and extracted)	0.25
S2p1a-s-2	Massive slag (melt cooled down in pit furnace)	1.58
S2p1a-sm	Mixture of slag and matte	0.35
S2p1b-sc-1	Matte, drilled from furnace conglomerate	0.42
S2p1b-sc-2	Matte, drilled from furnace conglomerate	−0.28
S2p1b-sc-3	Matte, drilled from furnace conglomerate	0.21
S2p1b-sc-4	Copper prill, extracted from furnace conglomerate	0.26
S2p1b-sc-5	Slag, drilled from furnace conglomerate	0.64
S2p1b-sc-6	Slag, drilled from furnace conglomerate	0.74
S2p1b-sc-7	Slag, drilled from furnace conglomerate	0.13
S2p1b-sc-8	Slag, drilled from furnace conglomerate	0.09
S2p2-sm-m	Matte close to slag, crushed from same piece as S2p2-sm-s	−0.05
S2p2-sm-s	Slag close to matte, crushed from same piece as S2p2-sm-m	0.30
S2p2-sm-um	Unreacted matte	0.35
S2p3-cp	Copper prill	0.21
S2p3-m	Matte	0.30
S2p3-s	Slag	0.45
S2p3-fm	Mixed material, too small to separate	0.17

(*Continues*)

Table 2 *(Continued)*

Sample ID	*Material*	$\delta^{65}Cu$
S2p3-cc	unburnt charcoal after experiment	0.24
S2p3c1-m	Matte	0.24
S2p3c1-s	Slag	0.45
S2p3c2-m	Matte	0.29
S2p3c2-s	Slag	0.47
S2p3c3-m	Matte	0.07
S2p3c3-s	Slag	0.29
S2p3c4-cu	Copper regulus	0.31
S2p3c4-m	Matte	0.29
S2p3r1-rm	Roasted matte	0.28
S2p3c4-s-1	Slag	0.28
S2p3c4-s-2	Copper prills in slag sample S2p3c4-s-1	0.30
Experiment series S4		
S4f1-cc	Charcoal leftover in furnace	0.20
S4f1-cp	Copper prills	0.08
S4f1-m	Matte, bulk sample	0.53
S4f1-m1	Matte	0.41
S4f1-m2-1	Matte	−0.04
S4f1-m2-2	Copper hair grown on sample S4f1-m2-1	0.19
S4f1-m4	Matte	0.49
S4f1-s	Slag	0.29
S4f1-sm	Mixture of slag and matte	0.14
S4f1-fm	Mixed material, too small to separate	0.00
S4f1-uo	Unreacted ore	0.38
S4f1-fl1-1	Furnace lining	−1.59
S4f1-fl2-1	Furnace lining	0.20
S4r1-rm	Roasted matte	0.06
S4p1-cp	Copper prills	0.26
S4p1-m-1	Matte	−0.07
S4p1-m-2	Copper sponge	0.27
S4p1-m-3	Matte	0.21
S4p1-m-4	Copper prill	0.24
S4p1-fm	Mixed material, too small to separate	0.30
S4p1-cc	unburnt charcoal after experiment	−0.89
S4p1-s2	Platy slag (melt quenched with water and extracted)	0.33
S4p1-s4	Platy slag (melt quenched with water and extracted)	0.24
S4p1-sm-1	Slag in direct contact with matte (quenched)	0.12
S4p1-sm-2	Mixture of slag and matte from the same piece such as S4p1-sm-1	0.54
S4p2-m	Matte	0.00
S4p2-s	Slag	−0.03
S4p2-fm	Mixed material, too small to separate	1.02
S4p2c1-cu	Copper regulus	0.27
S4p2c1-m	Matte	0.22
S4p2c1-s	Slag	0.27
S4p2r1-rm	Roasted matte	0.20
S4p2c2-s	Slag	0.15
S4p2c2-sm	Matte close to slag	0.12
S4p2c3-cu-1	Copper prill	0.16
S4p2c3-cu-2	Copper regulus	0.23
S4p2c3-sm	Matte close to slag	0.22
S4p2c3-s	Slag	0.63

Raw materials (Figs 1 and 3)

The Cu isotope composition of the used ore is within the typical isotope composition range of primary Cu ores (e.g., Mathur and Fantle 2015). Charcoal and softwood plot within the range of the unroasted ore. Manure used for the production of matte pellets for roasting, and the furnace lining (clay) have negative δ^{65}Cu values. Sand has a significant high positive δ-value, matching the overall picture of the partitioning of the Cu isotopes in soils, ores or mudstones through aqueous contribution (Moynier *et al*. 2017; Mathur *et al*. 2009a, 2010; Lv *et al*. 2016). Compared with the matte, the slag samples seem in general to be shifted towards slightly heavier (positive) values, which is in agreement with the enrichment of the heavier Cu isotope in the oxidized species predicted by the principles of stable isotope fractionation theory (Schauble 2004).

Results of the S2 experiment series in detail (Figs 1 and 2)

Sulphide shaft furnace experiment S2f1 As for the furnace conglomerate ('slag cake', sc) from experiment S2f1 (sulphide ore, shaft furnace experiment), the measured Cu, matte and slag portions range between 0.23 and −0.28 δ^{65}Cu. The Cu isotope composition of matte and slag portions, hence, is in general without significant difference. However, within their tight range, the furnace conglomerate (S2f1-sc) is isotopically more heterogeneous than the matte. In contrary, massive matte of experiment S2f1 (matte = m), which had segregated from the slag cake during cooling, is nearly identical with the original ore, but bulk matte and ore are more positive than matte sampled from the furnace conglomerate (Fig. 2).

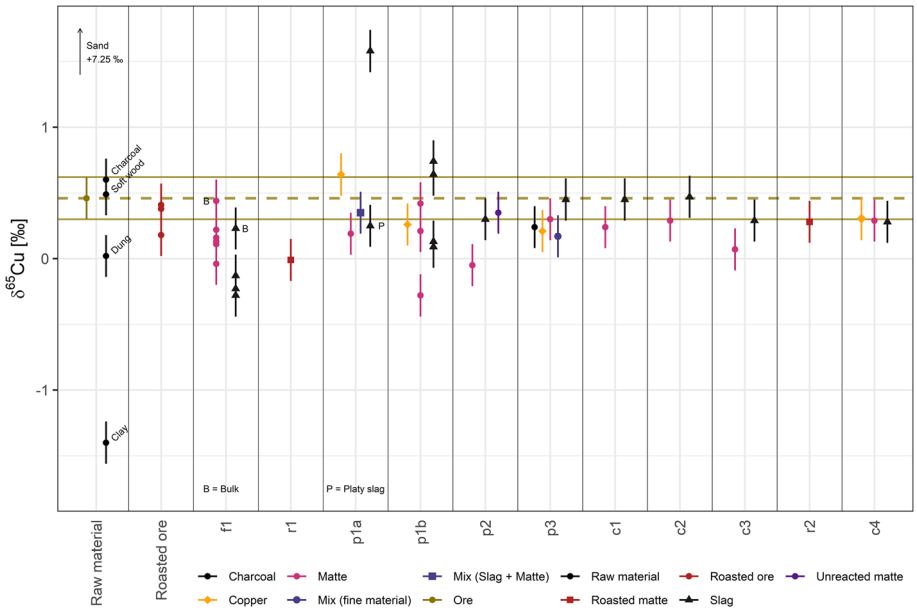

Figure 1 *Copper isotope signatures of the various samples of series S2: sulphide smelting in a shaft furnace and subsequent pit furnace and crucible smelting. As an anchor line, the isotopic composition of the ore is indicated by the band plotting slightly above zero (dashed line, solid lines = 2σ range). X-axis: various experiment installations and samples: f, furnace smelting; r, roasting; p, pit firing; c, crucible smelting. [Colour figure can be viewed at wileyonlinelibrary.com]*

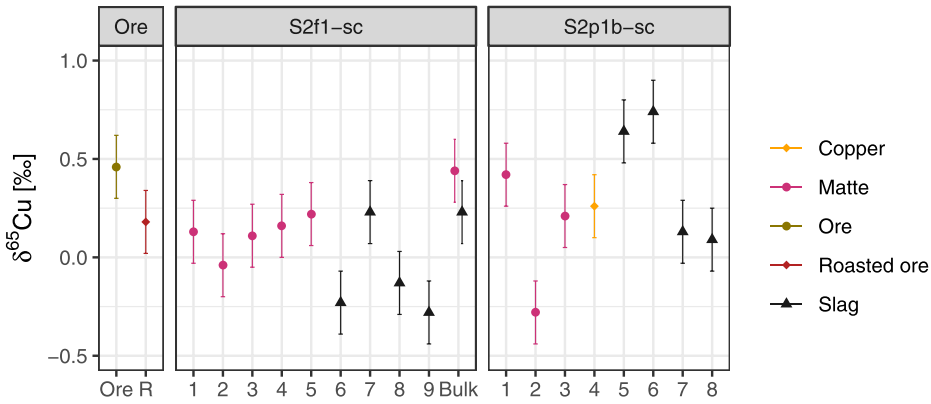

Figure 2 *Results of furnace conglomerates produced in series S2. Isotopically, inclusions of matte and copper are nearly identical. Matte and slag portions are in general without a large difference, but slag is isotopically more heterogeneous, whereas matte has a smaller range of variation. [Colour figure can be viewed at wileyonlinelibrary.com]*

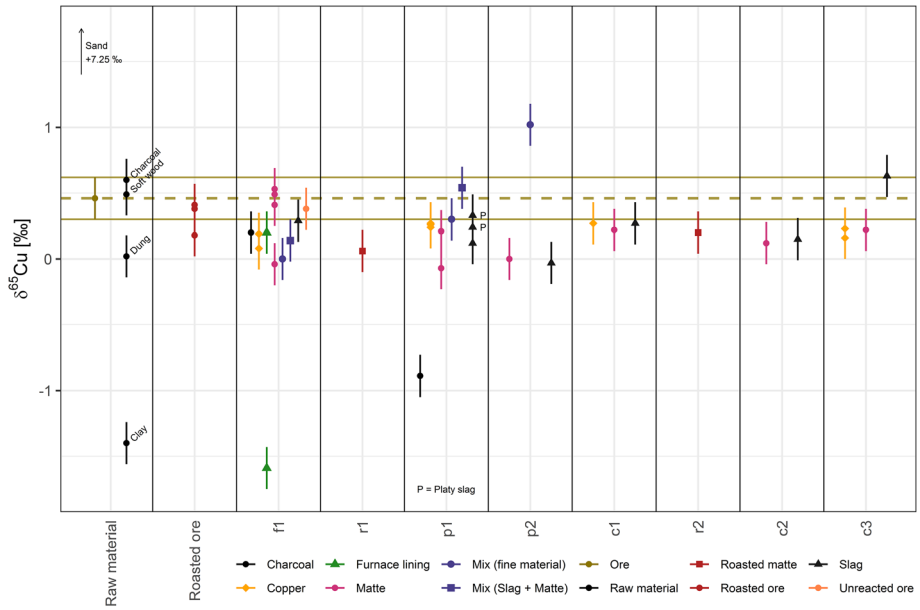

Figure 3 *Copper isotope signatures of the various samples of series S4: sulphide smelting in shaft furnace (f), pit furnace (p) and crucible (c). For abbreviations, cf. Figure 1. [Colour figure can be viewed at wileyonlinelibrary.com]*

Sulphide pit furnace experiment S2p1a (sulphide ore, pit furnace experiment) Part of the slag in this experiment was extracted as platy slag after rapid cooling (quenching) the surface of the molten mass with water. The other part of the slag (‘massive slag’) cooled down in the pit furnace. The crystallization grade of platy and massive slag is very different, and the massive slag contains nearly twice the amount of Cu than the platy slag (Table 1). The massive slag thus preferably traps Cu metal in the first place rather than platy slag, but according to their particular spatial position within the installation, density segregation forces the collection of the Cu metal in the

massive slag. Cu prills trapped in the massive slag have a slightly more positive (heavier) Cu isotope signature than matte inclusions and the massive slag itself. The Cu isotope signature of massive slag (S2p1a-s-2) is slightly heavier in isotope composition compared with the platy glassy slag (S2p1a-s-1). Mixed material of slag and matte ('fine material'; Table 2) is close to the ore.

Sulphide-pit furnace experiment S2p1b No bulk samples could be drawn, but the samples originating from different spots of the furnace conglomerate show a comparable spread of δ^{65}Cu in matte inclusions and slag with the matte tending to have lighter isotope compositions. The isotope composition of Cu prills in the slag does not differ from such of S2p1a.

Sulphide-pit furnace experiment S2p2 Comparably with S2p1, matte and slag are slightly different in their isotopic composition, with the slag being shifted towards heavier composition (more positive values).

Sulphide-pit furnace experiment S2p3 All materials have δ^{65}Cu signatures very close to each other, which means the absence of fractionation.

Crucible experiments and second matte roasting No changes in Cu isotopes occur.

Sulphide-pit furnace-crucible experiment S2p3c4

The matte from this experiment is very different in microstructure from the other mattes. The majority of mattes from the other experiments have a blocky microstructure with bluish-grey to brown-stained grains and are marbled by cracks. De-mixing structure is visible in the microscope, but more in the shape of stretch marks. Instead, this matte is very dense and fine-crystallized. The de-mixing structure is well oriented, and no silicate inclusions are present. Less Cu is precipitated. According to the chemical composition determined by -MS (Table 1) (Rose *et al*. 2020), the de-mixed composition is much lower in Fe content (1 wt%) than the blocky mattes (15–27 wt%). The same microstructure is only repeatedly seen in experiment S4p2c3, which is also a sulphide-pit furnace-crucible experiment after the second roasting of the matte. However, no significant differences can be detected isotopically between blocky and fine-crystallized matte.

Results of the S4 experiment series in detail (Fig. 3)

Sulphide-furnace experiment S4f1 All smelting-related materials have δ^{65}Cu signatures very close to each other, which means the absence of fractionation.

Sulphide-pit furnace experiment S4p1 Sulphide-pit furnace experiment S4p1 is an experiment, which produced a high portion of platy slag. A trend in the slag from the bottom to the top in favour of the heavier isotope can be seen, but all of them overlap in their analytical uncertainties, so that this does not necessarily represent an existing isotopic gradient.

Sulphide-pit furnace experiment S4p2 and crucible experiments The smelting products are all within the isotopic range of the other experiments. The mixed material of pit furnace experiment p2 (S4p2-fm) (Table 2) is isotopically heavier than matte and slag. The material from the second

matte roasting is close to the ore. Compared with the matte samples, the slag samples of the pit furnace experiments seem in general to be shifted towards slightly heavier values (experiments p2 and c1–c3). This slight trend can also be observed for pit furnace experiment S2p1b, although all samples lie within the general isotopic range.

DISCUSSION

The two experimental series showed that no significant total fractionation between the Cu ore and the smelted Cu metal could be detected. This is an important result for linking archaeological metal objects to their ore sources. However, when objects are not available for investigation, metallurgical by-products such as slags and matte, or their trapped metal inclusions, may also be seen as representative carriers of metal source information. For this reason, it is worthwhile to investigate the possible influence of the different components and raw materials more closely. Some possible fractionation phenomena can be uncovered that may not be considered at first. Because homogenization of the ore has been achieved before the analysis, Cu isotope mixing of the ore can be excluded (Fig. 4).

Organic contributions: Although the Cu content of wood and charcoal (Table 1) and thus their influence on the isotopic signature of Cu on the smelting assemblage might initially be assumed

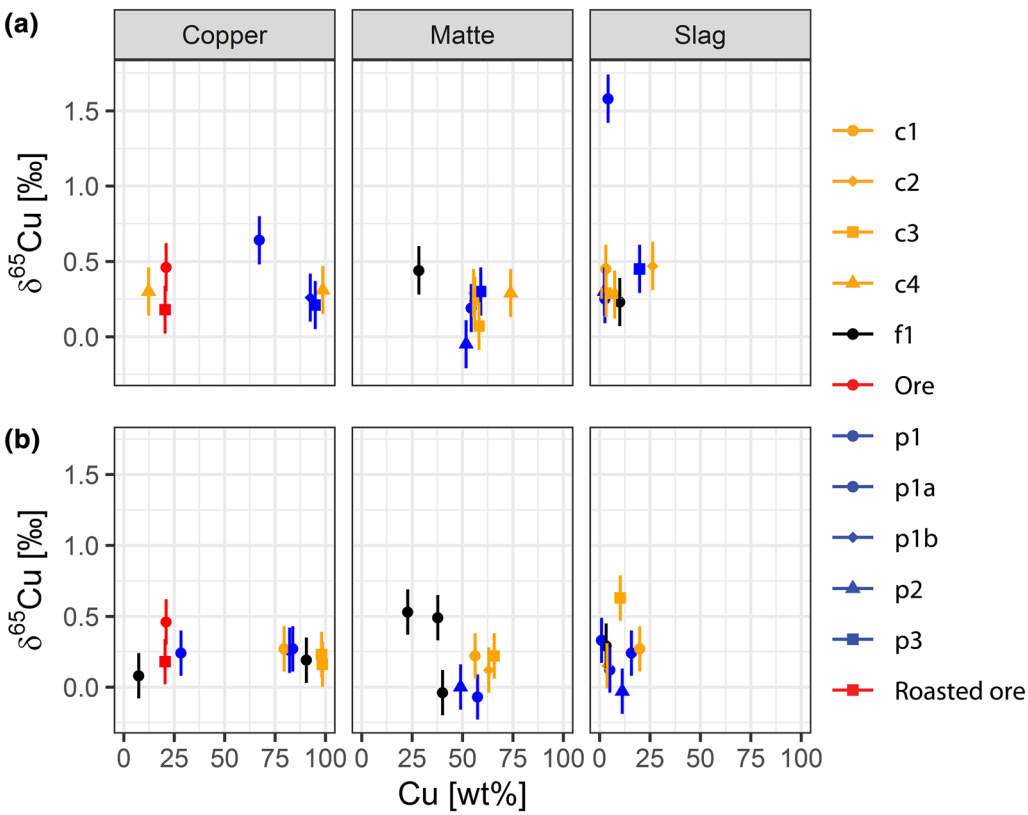

Figure 4 *Copper content (wt%) versus the copper isotope composition of the materials: (a) experiment series S2; and (b) experiment series S4. [Colour figure can be viewed at wileyonlinelibrary.com]*

to be negligible, the amount of fuel consumed is high and could add up its Cu traces over hours of stoking the fire. In each experiment, about 200 kg of wood were burnt in the shaft furnace, and 20 kg of roasted ore were introduced. The wood contained $< 0.005\%$ Cu by weight, while the charcoal contained 0.34% Cu by weight. In the end, the fuel may have the potential to affect the δ^{65}Cu signatures of the final products significantly. In the present case, the analyses have shown that both the wood and the charcoal used have Cu isotope signatures close to ore. This may differ for wood and charcoal from other trees or wood localities. The manure (< 0.005 wt % Cu) used in the experiments to form matte pellets was also tested, but is also isotopically insignificant.

Silica-rich contributions:

In the crucible experiments S2p3c1,2,3 and S4p2c1,3, the Cu isotopic signature of the slag is shifted towards heavier isotopic composition compared with the related matte, clearly beyond the overlapping analytical uncertainties of matte and slag. Sand was exclusively involved in these crucible experiments, which was intentionally added to produce slag. The Cu content of the sand used is 0.08 wt% Cu and contributes to the smelting assemblage with a heavy isotope ratio of 7.25 δ^{65}Cu. However, the measured values are exemplary here, as sand from other resources may have different Cu isotope values depending on its geological environment and sedimentary conditions (Wang *et al*. 2017). In sedimentary processes, fractionation effects occur due to the dissolution of Cu from rocks and its re-deposition, for example, as Cu silicate minerals in silica-rich sediments (Asael *et al*. 2007; Timna Cu ores). The Cu isotope composition of Timna sandstones shows more positive δ-values compared with Cu-rich primary quartz porphyries or secondary dolomites.

As for the shaft furnace experiments, no sand was added to the charge and this isotope effect is therefore not present. It is obvious that the isotopic composition of slag strongly coincides with the use of sand as a flux.

Contribution of clay from furnace lining or heat insulation of tuyères:

During the shaft furnace test S2f1 (but not during S4f1), the molten furnace wall dominated by its silica-rich clay component repeatedly clogged the tuyères. Continuous blowing and repositioning of the tuyères allowed to loosen and transport the clogging material towards their fire end. There, the clay most likely melted completely and homogenized with the slag. The lighter (more negative) δ^{65}Cu values of the slag in the experiment S2f1 compared with the matte and the absence of this effect in the experiment S4f1 can therefore be interpreted as a direct indicator of an isotopic impact of the clay used.

Loss of Cu through intentional cooling with water:

The roasting process of the ore caused a slight isotope shift from the ore signature to lighter (negative) values (Figs 1 and 3). This is probably not directly related to the oxidation process of the Cu sulphide minerals, but more likely due to a specific treatment. Owing to external factors the roasting reaction needed to be interrupted. This was achieved by quenching the material in water. The water quickly became greenish and bluish, indicating a considerable loss of Cu into the liquids (Fig. 5). Preferably, the isotopically heavier Cu dissolves in the aqueous phase and thus leads to fractionation with the heavier isotope (^{65}Cu) enriched in the solution (Wang

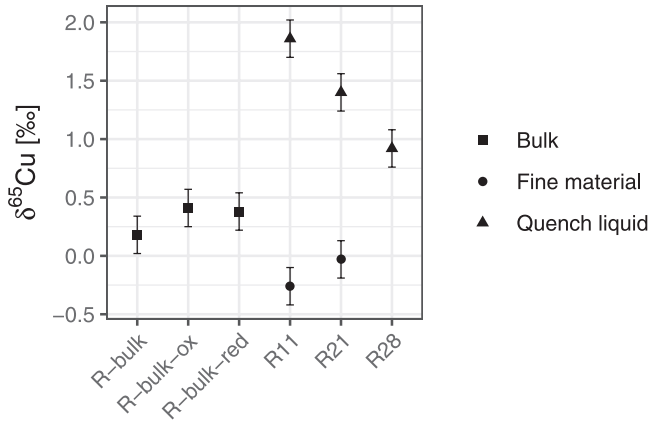

Figure 5 *Effect of quenching on the roasted ore. Clearly visible is a heavier isotope composition of the quenching liquids compared with the bulk ore, although the ore was very quickly removed from the water. Fractionation is even larger for samples R11 and R21. Here the water was in contact with small-grained roasted ore for several months. R-bulk = roasted ore, bulk sample; R-bulk-ox = roasted ore, bulk sample, oxidized portion; R-bulk-red = roasted ore, bulk sample, reduced portion; R11, 21, 28 = roasted ore samples.*

et al. 2017). It has to be emphasized that this fractionation effect cannot be generalized for all smelting processes, but is rather related to the specific conditions of the experiments.

Thermal diffusion and crystallization effects:

In experiment S2p1a, the molten mass was subjected to rapid cooling by sprinkling with water, thus forming a comparably thin, plate-like slag layer on top. The sprinkling with water using a bundle of water-soaked grass is known as a practice in smelting procedures from ethnological studies (Anfinset 2011). The platy slag withdrawn from the remaining molten mass portion, which later solidified as massive slag and matte, is thin, glassy and very fragile, while the massive slag formed as a thick cake in the hotter zone of the pit furnace. Owing to the much slower cooling rate, the massive slag is partially crystallized, compact and mechanically stable. The Cu isotopic composition of the platy slag is close to that of the matte, while the massive slag has a heavier Cu isotopic composition than the matte.

A possible explanation for the Cu isotope fractionation between matte, platy and massive slag could be a temperature dependence. Diffusion-induced fractionation takes place between the cooler and hotter regions of the molten slag, resulting in a growth-rate effect and significant fractionation of the stable metal isotopes (Richter *et al*. 2009; Williams and Archer 2011). According to Zhao *et al*. (2017), thermal diffusion enriches the heavier Cu isotope in the hotter region. At the same time, the heavier Cu isotopes in the crystal-rich regions are also enriched (stiffer bonds; Schauble 2004). It is difficult to estimate the temperature distribution in the melt, especially due to the exothermic reaction of the sulphides, but it is plausible that the molten slag is hotter near the sulphide-rich matte in the furnace and cooler towards the surface-exposed upper zone where the platy slag has formed.

As can be seen under the microscope, the effects of temperature gradation within the melt even have microstructural dimensions and are complex. Charcoal residues, certainly hotspots at the time of the start of cooling, drift forward a matte front, initially in the molten state, while at some

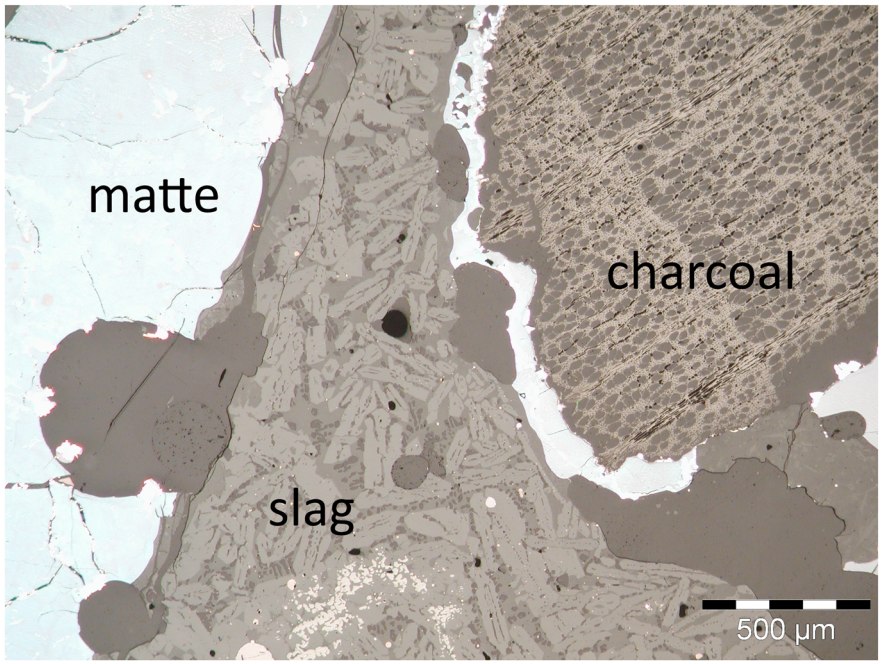

Figure 6 *Experiment S4p2-m: matte (light grey areas) with glassy and crystallized slag portions (grey laths and glassy structure) and charcoal (cellular structure). Cooling progresses gradually, resulting in cooler zones that allow crystals to grow slowly, and hotter zones close to the charcoal fragments. [Colour figure can be viewed at wileyonlinelibrary.com]*

distance the molten slag slowly begins to cool down, indicated by larger crystals (Fig. 6). Presumably, after the charcoal heat has died down and as a very last solidification phase, glassy or microcrystallized slag constituents quickly filled the remaining spaces between charcoal-matte areas and clusters of crystallized slag. This is the moment when the matte also cools and crystallizes. The slow cooling and constant crystal growth inside the slag cake, with or without coal inclusions, allows a continuous fractionation of the melt between crystallized and molten portions, that is, between matte and solid slag. Parallels in nature may be sought in layered intrusions with their differentiation and diffusion processes (e.g., Savage *et al*. 2015; Zhao *et al*. 2017), but the dimensions are by no means comparable. The fractionation effect within the massive slag enriches the heavier Cu isotope in the slag, while the rapid cooling of the surface-near platy slag prevented from fractionation of the material. The massive slag, therefore, has a heavier Cu isotope composition than the matte, while the platy slag is without fractionation and, thus, has an isotope signature comparable to that of the matte. The latter is obviously dominated exclusively by processes within the silicate slag melt and is decoupled from the sulphide-silicate (matte-slag) interactions.

This interpretation is reinforced by the observation in experiment S4p1, where the melt was much hotter (1200°C instead of < 800°C), and the liquid had a very low viscosity. The molten slag was quenched, which caused the melt to solidify immediately, and the solidified slag was completely removed and thus separated from the matte. Thermal diffusion and crystallization effects, and in consequence fractionation effects could not occur.

CONCLUSIONS

The fractionation of Cu isotopes between ore and produced Cu metal is not particularly evident from the experiments. Natural ore and roasted ore have Cu isotope signatures within the same small range of the majority of the other materials involved in the smelting procedure. Wood and charcoal, which were used for firing, also range within the small general Cu isotope range (Table 2 and Figs 1 and 3). Sand and furnace lining and especially their Cu content demonstrably influence the Cu isotope signature of the slag components.

From the detailed observations made, fractionation of Cu isotopes during smelting still needs to be considered for such smelting processes, which are suspected to have run under more uncontrolled/oxidative conditions. Because of generally unknown raw materials used for prehistoric smelting processes, the conditions need to be reconstructed in very detail for each single archaeological case, distinguishing the region, its geological setting, ore composition, and the necessity for fluxes. The fractionation of Cu isotopes also needs to be considered relevant in the context of the slag formation whenever the slag contains multiple phases or even charcoal inclusions, which cause heterogenous temperature zones with different cooling rates. In particular, the cooling rate, crystal growth and temperature gradient (massive slag versus platy slag, crystallized versus glassy slags, surficial layers versus slag cakes) have to be evaluated.

For these reasons, Cu isotope fractionation effects are potentially relevant, whenever (1) a high Cu concentration in slag remained, (2) the extraction of Cu prills out of highly viscous slag is suspected as a procedure of initial production or (3) the reworking of older slag is assumed. In the case of such Cu extraction procedures, Cu isotope fractionation can occur and may have influence on the provenancing of raw material through a comparison of produced Cu metal with ore.

ACKNOWLEDGEMENTS

The research project was funded by the Deutsche Forschungsgemeinschaft (DFG). The FIERCE is financially supported by the Wilhelm and Else Heraeus Foundation and by the DFG (INST 161/921-1 FUGG and INST 161/923-1 FUGG), which is gratefully acknowledged. The authors thank Dr H.-Michael Seitz and Serafina Endress for assistance during copper isotope analysis. This is the FIERCE contribution no. **7**. The RGZM Mainz was generous with its facilities at the LEA, Mayen; and Michael Herdick is thanked. Without the experienced skills of Erica Hanning and the helping hands of volunteer students, there would have been no smelting products to analyse. The electron microprobe was used at the Geowissenschaftliches Zentrum Göttingen with the help of Dr Andreas Kronz. At DBM, the authors thank Dr Michael Bode, Andreas Ludwig, Sandra Kruse, Georg Wange, Regina Kutz, Stephanie Menic, Isika Heuchel-Pede and Peter Thomas. Data were processed and plots created with R (R Core Team 2019) in RStudio®. The authors are grateful to the reviewers for substantial improvements to the paper.

REFERENCES

Albarède, F., 2004, The stable isotope geochemistry of copper and zinc, *Reviews in Mineralogy and Geochemistry*, **55**, 409–27. https://doi.org/10.2138/gsrmg.55.1.409.

Albarède, F., Albalat, E., and Télouk, P., 2015, Instrumental isotope fractionation in multiple-collector ICP-MS, *Journal of Analytical Atomic Spectrometry*, **30**, 1736–42. https://doi.org/10.1039/C5JA00188A.

Albarède, F., and Beard, B., 2004, Analytical methods for non-traditional isotopes, *Reviews in Mineralogy and Geochemistry*, **55**, 113–52. https://doi.org/10.2138/gsrmg.55.1.113.

Anfinset, N., 2011, *Social and technological aspects of mining, smelting and casting copper: An ethnoarchaeological study from Nepal*, 181, Veröffentlichungen aus dem Deutschen Bergbau-Museum Bochum, Bochum.

Arndt, N., and Fowler, A., 2004, Textures in komatiites and variolitic basalts, in *The Precambrian earth: Tempos and events*, 298–311, Elsevier, Amsterdam.

Artioli, G., Baumgarten, B., Morelli, M., Gussani, B., Recchia, S., Nimis, P., Giunti, I., Angelini, I., and Omenetto, P., 2008, Chemical and isotopic tracers in Alpine copper deposits: Geochemical links between mines and metals, *Geo. Alp*, **5**, 139–48.

Asael, D., 2010, Copper stable isotope fractionation in low-temperature geological systems (PhD thesis). Hebrew University of Jerusalem, Jerusalem, Israel.

Asael, D., Matthews, A., Bar-Matthews, M., and Halicz, L., 2007, Copper isotope fractionation in sedimentary copper mineralization (Timna Valley, Israel), *Chemical Geology*, **243**, 238–54. https://doi.org/10.1016/j.chemgeo.2007.06.007.

Bernhard, J., 1965, Die Mitterberger Kupferkieslagerstätte. Erzführung und Tektonik, *Jahrbuch der Geologischen Bundesanstalt*, **109**, 3–90.

Bigalke, M., Weyer, S., and Wilcke, W., 2010, Stable copper isotopes: A novel tool to trace copper behavior in hydromorphic soils, *Soil Science Society of America Journal*, **74**, 60–73.

Borrok, D. M., Nimick, D. A., Wanty, R. B., and Ridley, W. I., 2008, Isotopic variations of dissolved copper and zinc in stream waters affected by historical mining, *Geochimica et Cosmochimica Acta*, **72**, 329–44. https://doi.org/10.1016/j.gca.2007.11.014.

Bower, N. W., Hendin, D. B., Lundstrom, C. C., Epstein, M. S., Keller, A. T., Wagner, A. R., and White, Z. R., 2013, 'Biblical' bronze coins: New insights into their timing and attribution using copper and lead isotopes, *Archaeological and Anthropological Sciences*, **5**, 287–98. https://doi.org/10.1007/s12520-012-0113-4.

Brown, H., and Inghram, M. G., 1947, The isotopic composition of meteoritic copper, *Physics Review*, **72**, 347. https://doi.org/10.1103/PhysRev.72.347.

Bugaj, U., Nejbert, K., Ilnicki, S., Wieciński, P., Onyszczuk, T., Garbacz, H., and Włodarczak, P., 2019, Copper sulphosalts in early metallurgy (2600–1900 BC) – Chemical–mineralogical investigation of artefacts from southern Poland, *Geol. Q.*, **63**, https://doi.org/10.7306/gq.1473.

Dekov, V. M., Rouxel, O., Asael, D., Hålenius, U., and Munnik, F., 2013, Native cu from the oceanic crust: Isotopic insights into native metal origin, *Chemical Geology*, **359**, 136–49. https://doi.org/10.1016/j.chemgeo.2013.10.001.

Desaulty, A.-M., Telouk, P., Albalat, E., and Albarède, F., 2011, Isotopic Ag-Cu-Pb record of silver circulation through 16th–18th century Spain, *Proceedings of the National Academy of Sciences*, **108**, 9002–7. https://doi.org/10.1073/pnas.1018210108.

Ehrlich, S., Butler, I., Halicz, L., Rickard, D., Oldroyd, A., and Matthews, A., 2004, Experimental study of the copper isotope fractionation between aqueous Cu(II) and covellite, CuS. *Chemical Geology*, **209**, 259–69. https://doi.org/10.1016/j.chemgeo.2004.06.010.

Erdmann, S., Scaillet, B., Martel, C., Cadoux, Anita, 2014, *Characteristic Textures of Recrystallized, Peritectic, and Primary Magmatic Olivine in Experimental Samples and Natural Volcanic Rocks, Journal of Petrology* **55**,12, 2014, 2377–402. https://doi.org/10.1093/petrology/egu060.

Ewald, H., 1944, Die relativen Isotopenhäufigkeiten und die Atomgewichte von Kupfer und ruthenium, *Zeitschrift für Physik*, **122**, 487–93. https://doi.org/10.1007/BF01342769.

Fernandez, A., and Borrok, D. M., 2009, Fractionation of cu, Fe, and Zn isotopes during the oxidative weathering of sulfide-rich rocks, *Chemical Geology*, **264**, 1–2. https://doi.org/10.1016/j.chemgeo.2009.01.024.

Fujii, T., Moynier, F., Abe, M., Nemoto, K., and Albarède, F., 2013, Copper isotope fractionation between aqueous compounds relevant to low temperature geochemistry and biology, *Geochimica et Cosmochimica Acta*, **110**, 29–44. https://doi.org/10.1016/j.gca.2013.02.007.

Gale, N. H., and Stos-Gale, Z. A., 1982, Bronze age copper sources in the Mediterranean: A new approach, *Science*, **216**, 11–19. https://doi.org/10.1126/science.216.4541.11.

Gale, N. H., Woodhead, A. P., Stos-Gale, Z. A., Walder, A., and Bowen, I., 1999, Natural variations detected in the isotopic composition of copper: Possible applications to archaeology and geochemistry, *International Journal of Mass Spectrometry*, **184**, 1–9. https://doi.org/10.1016/S1387-3806(98)14294-X.

Hanning, E., and Pils, R., 2011, Experimentelle Untersuchungen zur bronzezeitlichen Kupferverhüttung im ostalpinen Gebiet—Erste Ergebnisse, in *Die geschichte des Bergbaus in Tirol und seinen angrenzenden Gebieten. Presented at the 5. Milestone-meeting des SFB HiMAT vom 7.–10.10.2010 in Mühlbach*, 129–34, Innsbruck University Press, Innsbruck, Mühlbach.

Hauptmann, A. (Ed.), 1989, Archäometallurgie der Alten welt: Beiträge zum Internationalen symposium 'Old World Archaeometallurgy', Heidelberg 1987 = Old world archaeometallurgy, Der Anschnitt Beiheft. Dt. Bergbau-Museum, Bochum.

Hauptmann, A., 2007, *The archaeometallurgy of copper: Evidence from Faynan, Jordan; with 40 tables*, Springer, Berlin.

Hauptmann, A., Pernicka, E., and Wagner, G.A., 1985, 5000 [Fünftausend] Jahre Kupfer in Oman. 1: Die Entwicklung der Kupfermetallurgie vom 3. Jahrtausend bis zur Neuzeit, Der Anschnitt. Vereinigung d. Freunde von Kunst u. Kultur im Bergbau, Bochum.

Herzog, G. F., Moynier, F., Albarède, F., and Berezhnoy, A. A., 2009, Isotopic and elemental abundances of copper and zinc in lunar samples, Zagami, Pele's hairs, and a terrestrial basalt, *Geochimica et Cosmochimica Acta*, **73**, 5884–904. https://doi.org/10.1016/j.gca.2009.05.067.

Huang, J., Huang, F., Wang, Z., Zhang, X., and Yu, H., 2017, Copper isotope fractionation during partial melting and melt percolation in the upper mantle: Evidence from massif peridotites in Ivrea-Verbano zone, Italian Alps, *Geochimica et Cosmochimica Acta*, **211**, 48–63. https://doi.org/10.1016/j.gca.2017.05.007.

Hull, S., Fayek, M., Mathien, F. J., and Roberts, H., 2014, Turquoise trade of the ancestral Puebloan: Chaco and beyond, *Journal of Archaeological Science*, **45**, 187–95. https://doi.org/10.1016/j.jas.2014.02.016.

Jansen, M., 2011, Möglichkeiten und Grenzen der cu-Isotopie in der Archäometallurgie des Kupfers. unpublished Master thesis Ruhr-University Bochum.

Jansen, M., Hauptmann, A., Klein, S., and Seitz, H.-M., 2018, The potential of stable cu isotopes for the identification of bronze age ore mineral sources from Cyprus and Faynan: Results from Uluburun and Khirbat Hamra Ifdan, *Archaeological and Anthropological Sciences*, **10**, 1485–502. https://doi.org/10.1007/s12520-017-0465-x.

Klein, S., Brey, G. P., Durali-Müller, S., and Lahaye, Y., 2010, Characterisation of the raw metal sources used for the production of copper and copper-based objects with copper isotopes, *Archaeological and Anthropological Sciences*, **2**, 45–56. https://doi.org/10.1007/s12520-010-0027-y.

Klein, S., Lahaye, Y., Brey, G. P., and von Kaenel, H.-M., 2004, The early roman imperial AES coinage II: Tracing the copper sources by analysis of lead and copper isotopes—copper coins of Augustus and Tiberius, *Archaeometry*, **46**, 469–80. https://doi.org/10.1111/j.1475-4754.2004.00168.x.

Larson, P. B., Maher, K., Ramos, F., Chang, Z., Gaspar, M., and Meinert, L. D., 2003, Copper isotope ratios in magmatic and hydrothermal ore-forming environments, *Chemical Geology*, **11**, 337–50.

Lechtman, H., and Klein, S., 1999, The production of copper-arsenic alloys (arsenic bronze) by cosmelting: Modern experiment, ancient practice, *Journal of Archaeological Science*, **26**, 497–526.

Lobo, L., Degryse, P., Shortland, A., Eremin, K., and Vanhaecke, F., 2014, Copper and antimony isotopic analysis via multi-collector ICP-mass spectrometry for provenancing ancient glass, *J Anal Spectrom*, **29**, 58–64. https://doi.org/10.1039/C3JA50303H.

Lv, Y., Liu, S.-A., Zhu, J.-M., and Li, S., 2016, Copper and zinc isotope fractionation during deposition and weathering of highly metalliferous black shales in Central China, *Chemical Geology*, **422**, 82. https://doi.org/10.1016/j.chemgeo.2015.12.017.

Maréchal, C., and Albarède, F., 2002, Ion-exchange fractionation of copper and zinc isotopes, *Geochimica et Cosmochimica Acta*, **66**, 1499–509. https://doi.org/10.1016/S0016-7037(01)00815-8.

Maréchal, C. N., Télouk, P., and Albarède, F., 1999, Precise analysis of copper and zinc isotopic compositions by plasma-source mass spectrometry, *Chemical Geology*, **156**, 251–73. https://doi.org/10.1016/S0009-2541(98)00191-0.

Markl, G., Lahaye, Y., and Schwinn, G., 2006, Copper isotopes as monitors of redox processes in hydrothermal mineralization, *Geochimica et Cosmochimica Acta*, **70**, 4215–28. https://doi.org/10.1016/j.gca.2006.06.1369.

Mason, T. F. D., Weiss, D. J., Horstwood, M., Parrish, R. R., Russell, S. S., Mullane, E., and Coles, B. J., 2004, High-precision cu and Zn isotope analysis by plasma source mass spectrometry, *Journal of Analytical Atomic Spectrometry*, **19**, 209. https://doi.org/10.1039/b306958c.

Mathur, R., Dendas, M., Titley, S., and Phillips, A., 2010, Patterns in the copper isotope composition of minerals in porphyry copper deposits in southwestern United States, *Economic Geology*, **105**, 1457–67. https://doi.org/10.2113/econgeo.105.8.1457.

Mathur, R., and Fantle, M. S., 2015, Copper isotopic perspectives on supergene processes: Implications for the global cu cycle, *Elements*, **11**, 323–9. https://doi.org/10.2113/gselements.11.5.323.

Mathur, R., Ruiz, J., Titley, S., Liermann, L., Buss, H., and Brantley, S., 2005, Cu isotopic fractionation in the supergene environment with and without bacteria, *Geochimica et Cosmochimica Acta*, **69**, 5233–46. https://doi.org/10.1016/j.gca.2005.06.022.

Mathur, R., Titley, S., Barra, F., Brantley, S., Wilson, M., Phillips, A., Munizaga, F., Maksaev, V., Vervoort, J., and Hart, G., 2009a, Exploration potential of cu isotope fractionation in porphyry copper deposits, *Journal of Geochemical Exploration*, **102**, 1–6. https://doi.org/10.1016/j.gexplo.2008.09.004.

Mathur, R., Titley, S., Barra, F., Brantley, S., Wilson, M., Phillips, A., Munizaga, F., Makseav, V., Vervoort, J., and Hart, G., 2009b, Copper isotope fractionation used to identify supergene processes, in: Special publication. Pp. 43–49.

Mathur, R., Titley, S., Hart, G., Wilson, M., Davignon, M., and Zlatos, C., 2009c, The history of the United States cent revealed through copper isotope fractionation, *Journal of Archaeological Science*, **36**, 430–3. https://doi.org/10.1016/j.jas.2008.09.029.

Mathur, R., and Wang, D., 2019, Transition metal isotopes applied to exploration geochemistry: Insights from Fe, cu, and Zn, in *Geophysical monograph series* (eds. S. Decrée and L. Robb), 163–83, John Wiley & Sons, Inc., Hoboken, NJ, USA.

Moynier, F., Albarède, F., and Herzog, G. F., 2006, Isotopic composition of zinc, copper, and iron in lunar samples, *Geochimica et Cosmochimica Acta*, **70**, 6103–17. https://doi.org/10.1016/j.gca.2006.02.030.

Moynier, F., Blichert-Toft, J., Telouk, P., Luck, J.-M., and Albarède, F., 2007, Comparative stable isotope geochemistry of Ni, cu, Zn, and Fe in chondrites and iron meteorites, *Geochimica et Cosmochimica Acta*, **71**, 4365–79. https://doi.org/10.1016/j.gca.2007.06.049.

Moynier, F., Vance, D., Fujii, T., and Savage, P., 2017, The isotope geochemistry of zinc and copper, *Reviews in Mineralogy and Geochemistry*, **82**, 543–600. https://doi.org/10.2138/rmg.2017.82.13.

Ney, P., 1986, *Gesteinsaufbereitung im labor*, Enke, Stuttgart.

Peel, K., Weiss, D., Chapman, J., Arnold, T., and Coles, B., 2008, A simple combined sample–standard bracketing and inter-element correction procedure for accurate mass bias correction and precise Zn and cu isotope ratio measurements, *Journal of Analytical Atomic Spectrometry*, **23**, 103–10. https://doi.org/10.1039/B710977F.

Petit, J. C. J., de Jong, J., Chou, L., and Mattielli, N., 2008, Development of cu and Zn isotope MC-ICP-MS measurements: Application to suspended particulate matter and sediments from the Scheldt estuary, *Geostandards and Geoanalytical Research*, **32**, 149–66. https://doi.org/10.1111/j.1751-908X.2008.00867.x.

Pokrovsky, O. S., Viers, J., Emnova, E. E., Kompantseva, E. I., and Freydier, R., 2008, Copper isotope fractionation during its interaction with soil and aquatic microorganisms and metal oxy (hydr)oxides: Possible structural control, *Geochimica et Cosmochimica Acta*, **72**, 1742–57. https://doi.org/10.1016/j.gca.2008.01.018.

Powell, W., Mathur, R., Bankoff, H. A., Mason, A., Bulatović, A., Filipović, V., and Godfrey, L., 2017, Digging deeper: Insights into metallurgical transitions in European prehistory through copper isotopes, *Journal of Archaeological Science*, **88**, 37–46. https://doi.org/10.1016/j.jas.2017.06.012.

R Core Team 2019, *R: A Language and Environment for Statistical Computing, R Foundation for Statistical Computing*, Vienna, Austria.

Reguera-Galan, A., Barreiro-Grille, T., Moldovan, M., Lobo, L., Blas Cortina, M. Á., and García Alonso, J. I., 2019, A provenance study of early bronze age artefacts found in Asturias (Spain) by means of metal impurities and Lead, copper and antimony isotopic compositions, *Archaeometry*, **61**, 683–700. https://doi.org/10.1111/arcm.12445.

Richter, F. M., Dauphas, N., and Teng, F.-Z., 2009, Non-traditional fractionation of non-traditional isotopes: Evaporation, chemical diffusion and Soret diffusion, *Chemical Geology*, **258**, 92–103. https://doi.org/10.1016/j.chemgeo.2008.06.011

Rose, T., Hanning, E., and Klein, S., 2019, Verhüttungsexperimente mit Chalkopyrit-Erz nach Vorbildern aus dem bronzezeitlichen Ostalpenraum und Nepal, *Exp. Archäol. Eur. Jahrb.*, **18**, 47–60. https://doi.org/10.23689/fidgeo-3706.

Rose, T., Morgenstern, G., Stelter, M., and Klein, S, 2017, Cu isotope fractionation during prehistoric smelting: A contribution of modern pyrometallurgy., in: Proceedings of the European Metallurgical Conference 2017. Presented at the European Metallurgical Conference, Clausthal-Zellerfeld, pp. 1153–67.

Rose, Th., Klein, S., and Hanning, E., 2020, Rose, Thomas; Klein, Sabine; Hanning, Erica K. (2020): Copper isotope fractionation during prehistoric smelting of copper sulfides: Experimental and analytical data. GFZ data services. https://doi.org/10.5880/fidgeo.2020.013

Savage, P. S., Moynier, F., Chen, H., Shofner, G., Siebert, J., Badro, J., and Puchtel, I. S., 2015, Copper isotope evidence for large-scale sulphide fractionation during Earth's differentiation, *Geochemical Perspectives Letters*, 53–64. https://doi.org/10.7185/geochemlet.1506.

Schauble, E. A., 2004, Applying stable isotope fractionation theory to new systems, *Reviews in Mineralogy and Geochemistry*, **55**, 65–111. https://doi.org/10.2138/gsrmg.55.1.65.

Shields, W. R., Goldich, S. S., Garner, E. L., and Murphy, T. J., 1965, Natural variations in the abundance ratio and the atomic weight of copper, *Journal of Geophysical Research*, **70**, 479–91. https://doi.org/10.1029/JZ070i002p00479.

Vance, D., Archer, C., Bermin, J., Perkins, J., Statham, P. J., Lohan, M. C., Ellwood, M. J., and Mills, R. A., 2008, The copper isotope geochemistry of rivers and the oceans, *Earth and Planetary Science Letters*, **274**, 204–13. https://doi.org/10.1016/j.epsl.2008.07.026.

Walker, E. C., Cuttitta, F., and Senftle, F. E., 1958, Some natural variations in the relative abundance of copper isotopes, *Geochimica et Cosmochimica Acta*, **15**, 183–94. https://doi.org/10.1016/0016-7037(58)90056-5.

Wang, Z., Chen, J., and Zhang, T., 2017, Cu isotopic composition in surface environments and in biological systems: A critical review, *International Journal of Environmental Research and Public Health*, **14**, 538. https://doi.org/10.3390/ijerph14050538.

White, F. A., Sheffield, J. C., and Rourke, F. M., 1962, Isotopic abundance determination of copper by sputtering, *Journal of Applied Physics*, **33**, 2915–2915. https://doi.org/10.1063/1.1702590.

Williams, H. M., and Archer, C., 2011, Copper stable isotopes as tracers of metal–sulphide segregation and fractional crystallisation processes on iron meteorite parent bodies, *Geochimica et Cosmochimica Acta*, **75**, 3166–78. https://doi.org/10.1016/j.gca.2011.03.010.

Woodhead, A. P., Gale, N. H., and Stos-Gale, Z. A., 1999, An investigation into the fractionation of copper isotopes and its possible application to archaeometallurgy, in *Metals in antiquity. Presented at the international symposium at Harvard University from 10 to 13 September 1997, British archaeological reports*, 134–9, International Series, Archaeopress, Oxford.

Zhao, Y., Xue, C., Liu, S.-A., Symons, D. T. A., Zhao, X., Yang, Y., and Ke, J., 2017, Copper isotope fractionation during sulfide-magma differentiation in the Tulaergen magmatic Ni–cu deposit, NW China, *Lithos*, **286–287**, 206–15. https://doi.org/10.1016/j.lithos.2017.06.007.

Zhu, X. K., O'Nions, R. K., Guo, Y., Belshaw, N. S., and Rickard, D., 2000, Determination of natural Cu-isotope variation by plasma-source mass spectrometry: Implications for use as geochemical tracers, *Chemical Geology*, **163**, 139–49. https://doi.org/10.1016/S0009-2541(99)00076-5.